FERMILAB-FN-0816-E

Available on CMS information server

CMS NOTE 2007/021

The Compact Muon Solenoid Experiment

CMS Note

Mailing address: CMS CERN, CH-1211 GENEVA 23, Switzerland

August 17, 2007

Beam Position Determination using Tracks

T. Miao, H. Wenzel, F. Yumiceva

Fermilab, Batavia, USA

N. Leioatts

Florida Institute of Technology, Melbourne, USA

Abstract

Track-based algorithms to determine the LHC beam position and profile at the CMS collision point are described. Only track information is used and no reconstruction of the primary event vertex is required. With only about one thousand tracks, a statistical precision of 2 μm for the transverse beam position is achieved, assuming a well aligned detector. The algorithms are simple and fast, and can be used to monitor the beam in real time. A method to determine the track impact parameter resolution using the beam position and beam width calculation is also presented.

1 Introduction and Motivation

The collision region provides a very precise reference point in the plane transverse to the beam axis. The width of the beam in the CMS interaction region is expected to be around 16 μm for nominal physics operation and the expected variation of the beam during the beam coast, which should last on order of 10 hours, is expected to be approximately 20% of the beam width ([1] page 273). This makes the precise determination of the beam position an important input for many physics analysis [2]. In addition, this estimate can be used to check the tracking performance and to extract the average impact parameter resolution.

This note first describes methods to determine the beam position and profile. Once this information is known with high precision, it can be used to measure the average impact parameter resolution. Section 2 describes the different beam and tracking scenarios that have been considered in this study. Section 3 describes the two different methods to generate the Monte Carlo simulation samples. The first is a fast, parameterized Monte Carlo simulation using track resolutions from the full simulation. The fast Monte Carlo simulation allows one to study a large variety of beam and tracking parameterizations, but does not include effects like pattern recognition errors, noise, non-Gaussian tails etc. Therefore, for more realistic studies, the full GEANT 4 based simulation of the CMS detector was used, followed by the full reconstruction. Section 4 describes the $d_0 - \varphi_0$ fitter which is used to determine the position and slopes of the beams and Section 5 describes additional fitting routines which extend the $d_0 - \varphi_0$ fitter to extract additional information about the beam. All the fitting routines are track based, requiring no reconstruction of the primary event vertex. In Section 6, the beam parameters are assumed to be known with high precision and this information is used to measure the impact parameter resolution function.

Some reasons why the precise determination of the beam position and other beam parameters are so important are:

- They allow the beam position to be used, especially in the High Level Trigger (HLT), as a precise estimate of the primary interaction point for many physics analysis (lifetime, b-tagging, etc.). The beam position can be used as a constraint in a primary vertex finder to further improve the vertex precision.
- A beam-constraint can be used to improve the momentum resolution for tracks coming from the primary vertex (prompt tracks). They allow for unbiased pattern recognition (HLT and offline). In the pattern recognition, a beam constraint is used in the seed generation to form the initial track candidates. Although the beam constraint is removed in the final fit, a wrong beam position could bias the pattern recognition and lead to inefficiencies.
- They facilitate the determination of the track impact parameter resolution (see Section 6). This in turn allows one to validate the alignment and to check that the detector material is modeled correctly. The transverse beam width of $\approx 16\mu$m is smaller than the expected single track resolution even with the pixel system. This fact can be used to directly estimate the average single track impact parameter resolution of the Tracker. For high p_T tracks, the resolution will initially be dominated by the alignment of the detector; the beam width can therefore be used to directly check the alignment of the detector. Any new set of alignment parameters can be validated by demonstrating that the impact parameter distribution for prompt high p_T tracks gets narrower. Measuring how the impact parameter resolution varies with the track momentum is a measure of how well the contribution of multiple scattering to the track resolution and the material distribution in the Tracker is modeled.
- They permit a check of the global alignment and the relative position alignment between sub-systems of the CMS tracker. Using track stubs from different subsystems (TIB, TOB,TID, TEC, BPix and FPix) will allow the alignment of each sub-system with respect to the others (see e.g. [3] page 125).
- They provide a real time beam position monitoring for minimizing the radiation dose in the Tracker and feedback to the accelerator operators. To keep the exposure to ionizing radiation uniform in φ, it is desirable to keep the beam in the center of the tracking detector. Measurements by CDF have shown that the ionization radiation in the tracking volume has a radial dependence $\approx 1/r^{\alpha}$ with α in the range from 1.5 to 1.8. Here r is the radial distance from the beam [4].

2 Simulation of the Beam parameters and Tracker scenarios

2.1 Parameterization of the beam and different beam scenarios

At the LHC (pp) and the Tevatron ($p\bar{p}$), the longitudinal (along the beam direction) distribution of the collision region is fairly long and according to [5] can be parameterized by a Gaussian with a width of the order of 6 - 11

cm for CMS and 25 cm for CDF at the Tevatron. For both LHC and the Tevatron the transverse beam distributions are Gaussian, with widths of the order of 10 to 20 μm. In general, the beam width as a function of z is described by the so-called β-function (see, for example, [5] and [6]):

$$\sigma^b(z - z_0) = \sqrt{\epsilon \cdot \beta^* \cdot (1 + ((z - z_0)/\beta^*)^2)}, \tag{1}$$

where β^* is the amplitude function at the interaction point, ϵ is the emittance, and z_0 is the center of the longitudinal beam spot.

Table 1 lists the parameters for different beam scenarios that were evaluated. Figure 1 shows how the width of the beam σ^b varies as a function of z. The width of the beam varies by only a small amount in the nominal LHC configuration, while for the Tevatron Run II the beam width varies by about 10 μm between $z = -30$ and $z = 30$ cm. This feature enables CDF to measure not only the averaged beam position but also the β^* and ϵ parameters utilizing the excellent position resolution of its silicon system [2] [7].

Table 1: *Different beam scenarios.*

	β^* [cm]	ϵ [cm]	σ_z [cm]
Tevatron Run II [9] [10]	35	14 $\times 10^{-8}$	25
LHC start-up [1] [11]	200	3.75 $\times 10^{-8}$	11.24
LHC nominal [1] [11]	55	3.75 $\times 10^{-8}$	7.55

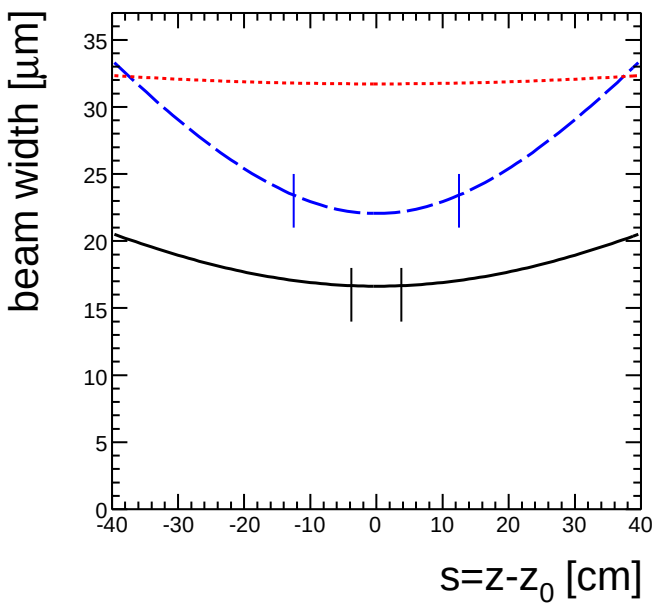

Figure 1: *Width of the beam as a function of z in cm for three different beam scenarios . The solid (black) line corresponds to the nominal LHC configuration. The fine dashed (red) line is a LHC fat beam at $\beta^* = 200$ cm and $\epsilon = 3.75 \times 10^{-8}$ cm. The dashed (blue) line corresponds to the Tevatron Run II beam configuration. The marks show the RMS of the collision region.*

2.2 Tracking detector resolution scenarios

The five parameter description of a track helix is: (C,φ_0,d_0,$\cot\theta$,z_p)

where:

C	:	is the half curvature of the track (same sign as the charge of the particle)
φ_0	:	is the direction of the track at point of minimum approach.
d_0	:	is the signed impact parameter distance between helix and origin at minimum approach.
$\cot\theta$	:	is the cotangent of the polar angle at minimum approach.
z_p	:	is the z position at minimum approach.

Two CMS detector configurations, as derived from full GEANT 4 simulations, are considered in this note: with pixels (see Ref. [1] page 256) and without pixels (Ref. [1] page 256 and Ref. [8]) in the tracking system. To be precise the configuration without pixels means the Pixel detector is in place but it is not being read out and therefore no pixel measurements contribute to the track fit. The material of the pixel layers still contributes to the multiple scattering and energy loss and therefore has to be taken into account. These two detector configurations have very different resolutions on the track parameters most relevant to the beam profile calculation: impact parameter d_0, φ_0 and z_0. The resolution function was parameterized as function of p_T (in GeV/c), ignoring any polar angle dependence,

$$\sigma_{d0}^{tr} = c_0 + \frac{c_1}{p_T}. \tag{2}$$

The parameter values are listed in Table 2 for d_0, φ_0 and z_0 for both scenarios. For comparison, resolutions from the CDF-II-like detector are also listed.

Table 2: *Resolution functions of two CMS detector configurations. For comparison, resolutions from the CDF-II-like detector are also listed.*

configuration	CMS with Pixel	CMS without pixel	CDF-II
d_0	$10 + 90/p_T$ (μ m)	$100 + 900/p_T$ (μm)	$11 + 10/p_T$ (μm)
φ_0	$0.00011 + 0.00190/p_T$ (rad)	$0.00023 + 0.00580/p_T$ (rad)	0.0003 (rad)
z_p	$0.0017 + 0.0084/p_T$ (cm)	$0.017 + 0.084/p_T$ (cm)	0.5 (cm)

3 Data Generation

3.1 Fast parameterized Monte Carlo simulation using `ROOT TPythia`

The parameterized Monte Carlo simulation uses the `ROOT TPythia` class [12], which provides a C++ interface to the F77 version of the `PYTHIA` 6.319 event generator [13]. This allows the fast generation of large data sets with different beam parameters and tracking scenarios. On an AMD64 (32Bit OS), the rate is 162 events/sec for minimum bias events compared to rates of the order of one event per minute for the full simulation. In the current form, the fast parameterized Monte Carlo simulation does not include any pattern recognition effects. `PYTHIA` creates interactions at the origin of the coordinate system. Final state charged particles are selected and the event vertex is distributed according to Equation (1); offsets in x and y are applied and the beam can have a slope in x and y with respect to the detector axis. Then the vertex and momentum information of these particles is transformed into helix track parameters.

The track parameters of interest are then resolution smeared according to the different track resolution scenarios described in Section 2.2.

Two sets of `PYTHIA` control cards were used:

1. Minimum bias.
2. QCD event with minimal parton E_T of 50 GeV/c.

More detail about the control cards can be found in Appendix 2. The rapidity and transverse momentum distributions of charged tracks are shown in Figure 2 for 10000 pp collisions for the two PYTHIA sets. The minimum bias events have very low multiplicity, yielding only 1 track with $p_T > 1.5$ GeV/c per event compared to about 7 such tracks for the events with the minimum parton E_T requirement.

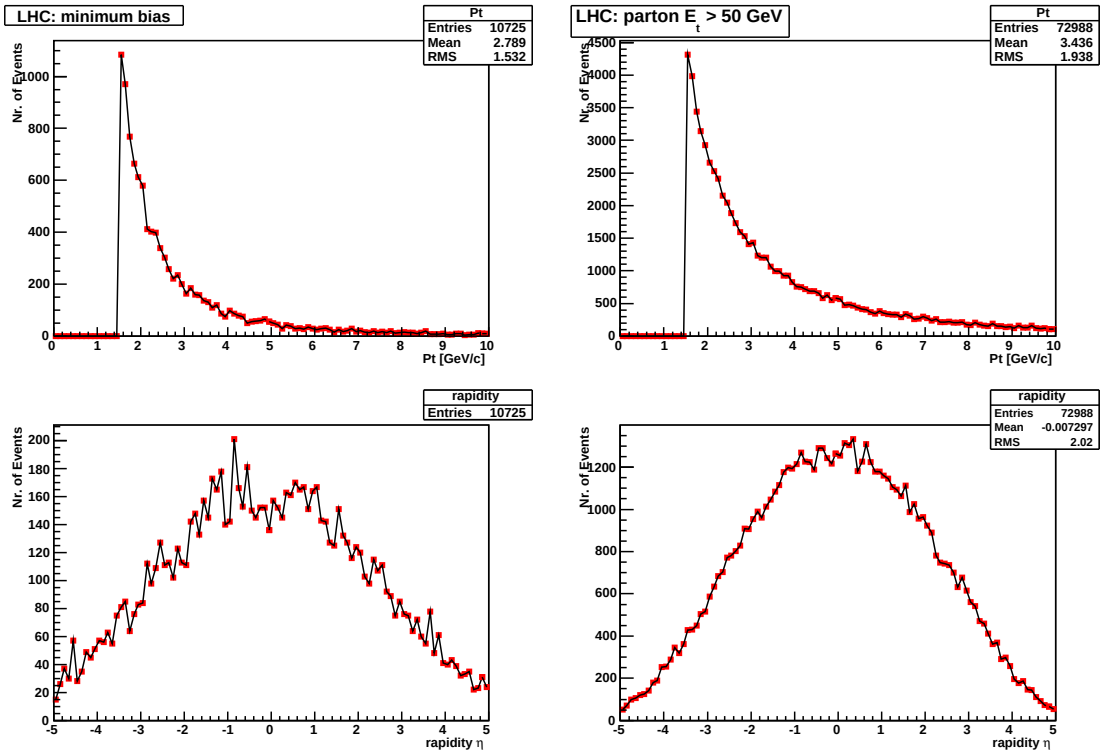

Figure 2: *Rapidity and p_T distribution of charged tracks for minimum bias events (left) and for events with a minimum parton E_T >50 GeV (right) at $\sqrt{s} = 14$ TeV. Only tracks with $p_T > 1.5$ GeV/c are considered.*

3.2 Full detector simulation and track reconstruction using `CMSSW`

In this case the full detector simulation based on GEANT 4 and the full reconstruction within the `CMSSW` framework is used to generate and reconstruct events. This gives a more realistic simulation, including pattern recognition effects, noise hits, non-Gaussian tails etc. Tracks from the Combinatorial Track Finder (CTF) [14] collection were used. The track selection requirements for fully reconstructed tracks are listed in Table 3.

The fully reconstructed samples used are QCD samples for several $\hat{p}_t$ bins and no pile-up, a QCD sample with low luminosity pile-up ($2 \times 10^{33} cm^{-2} s^{-1}$), an inclusive $b\bar{b}$ sample, and an inclusive $t\bar{t}$ sample. The QCD samples consist mainly of prompt tracks emanating from the primary interaction vertex, while $b\bar{b}$ and $t\bar{t}$ samples contain a significant amount of tracks with non-zero impact parameter stemming from displaced b-decays. We demonstrate that the $d_0 - \varphi_0$ fitter is insensitive to the sample composition. QCD samples with displaced beam spots were also produced (see Table 4).

In order to simulate a more realistic beam profile, a vertex smearing software module [15] based on the β-function was included. This smearing module displaces the vertex given by the generators using the β-function for the transverse coordinates and a Gaussian distribution for the longitudinal coordinate. This module also allows the beam to have slopes $\frac{dx}{dz}$ and $\frac{dy}{dz}$ with respect to the z-axis. The following parameters can be varied:

- `X0`, `Y0`, and `Z0`, where the default values are $(0, 0, 0)$ μm.
- `SigmaZ` (σ_z) with the default of 7.55 cm
- `dx/dz` and `dy/dz` where the default is 0 μm/cm .
- `BetaStar` (β^*) with a default of 55 cm.
- `Emittance` (ϵ) with a default of 3.75×10^{-8} cm.

Table 3: *Track selection requirements for fully simulated and reconstructed tracks.*

Silicon Strip Hits	> 7
Pixel Hits	> 1
$\chi^2/ndof$	< 5
transverse momentum (p_T)	> 2 GeV/c
impact parameter uncertainty (σ_{d0})	< 150 μm

4 The $d_0 - \varphi_0$ fitter

This fit is both fast and robust and has been in use by CDF for many years (see e.g. [3]) to estimate the beam positions both on-line and off-line. Within the CMS experiment, this fitter has also been initially studied [18]. Many physics analysis use the beam position calculated by this method as a precise unbiased estimate of the primary interaction vertex. This fitting method is also used to get the initial parameters for the other fitters described in Section 5.1. A determination of the primary vertices is not necessary for this algorithm and less data than fits based on reconstructed primary vertices is required. The algorithms are expected to be insensitive to pile up contributions, since it does not matter if the track emanates from the hard collision or from pile up. The various fitters were integrated into the CMS offline framework [16], but are also available as stand alone routines [17].

The variation of the impact parameter of all tracks is shown in Figures 3(a) and 3(c) as a function of φ when the beam is displaced with respect to the detector coordinate system. The transverse beam profile is shown in Figures 3(b) and 3(d). Figures 3(a) and 3(b) correspond to a high statistics sample obtained with the fast Monte Carlo simulation described in Section 3.1. The distributions corresponding to the fully simulated sample of 3000 minimum bias events are shown in Figures 3(c) and (d). The total number of tracks, selected by the requirements listed in Table 3, is 1268.

This correlation is used to extract the beam parameters. To first order, the impact parameter d_0 for tracks coming from the primary vertex can be parametrized by

$$d_0(\varphi_0, z_p) = x_0 \cdot \sin\varphi_0 + \frac{dx}{dz} \cdot \sin\varphi_0 \cdot z_p - y_0 \cdot \cos\varphi_0 - \frac{dy}{dz} \cdot \cos\varphi_0 \cdot z_p, \tag{3}$$

where x_0 and y_0 are the position of the beam at $z = 0$, and $\frac{dx}{dz}$ and $\frac{dy}{dz}$ are the x and y slopes of the beam.

The $d_0 - \varphi_0$ fitter is a simple iterative χ^2 fitter. The contribution from each track is weighted by its error. The χ^2 distribution to be minimized is

$$\chi^2 = \sum_{i=1}^{N_{Tracks}} \left(\frac{d_{0i} - (x_0 \cdot \sin\varphi_{0i} + \frac{dx}{dz} \cdot \sin\varphi_{0i} \cdot z_{pi} - y_0 \cdot \cos\varphi_{0i} - \frac{dy}{dz} \cdot \cos\varphi_{0i} \cdot z_{pi})}{\sigma_i} \right)^2, \tag{4}$$

where $\sigma_i^2 = \sigma_{d0}^2 + 2 \cdot \sigma_{Beam}^2$, and σ_{Beam} is the average transverse beam width.

Using a vector notation, the χ^2 function can be written as

$$\chi^2 = \sum_{i=1}^{N_{Tracks}} \left(\frac{d_{0i} - (\vec{x} \cdot \vec{g_i})}{\sigma_i} \right)^2, \tag{5}$$

where $\vec{x} = (x_0, y_0, \frac{dx}{dz}, \frac{dy}{dz})$ and $\vec{g_i} = (\sin\varphi_{0i}, -\cos\varphi_{0i}, \sin\varphi_{0i} \cdot z_{pi}, -\cos\varphi_0 \cdot z_p)$.

The solution for $\vec{x}$ is then

$$\vec{x} = V \cdot \vec{sg}, \tag{6}$$

where the inverse of the 4×4 matrix V is given by

$$V_{lm}^{-1} = \sum_{i=1}^{N_{Tracks}} \frac{g_{il} \cdot g_{mi}}{\sigma_i^2}, \quad (l, m = 1, 2, 3, 4) \tag{7}$$

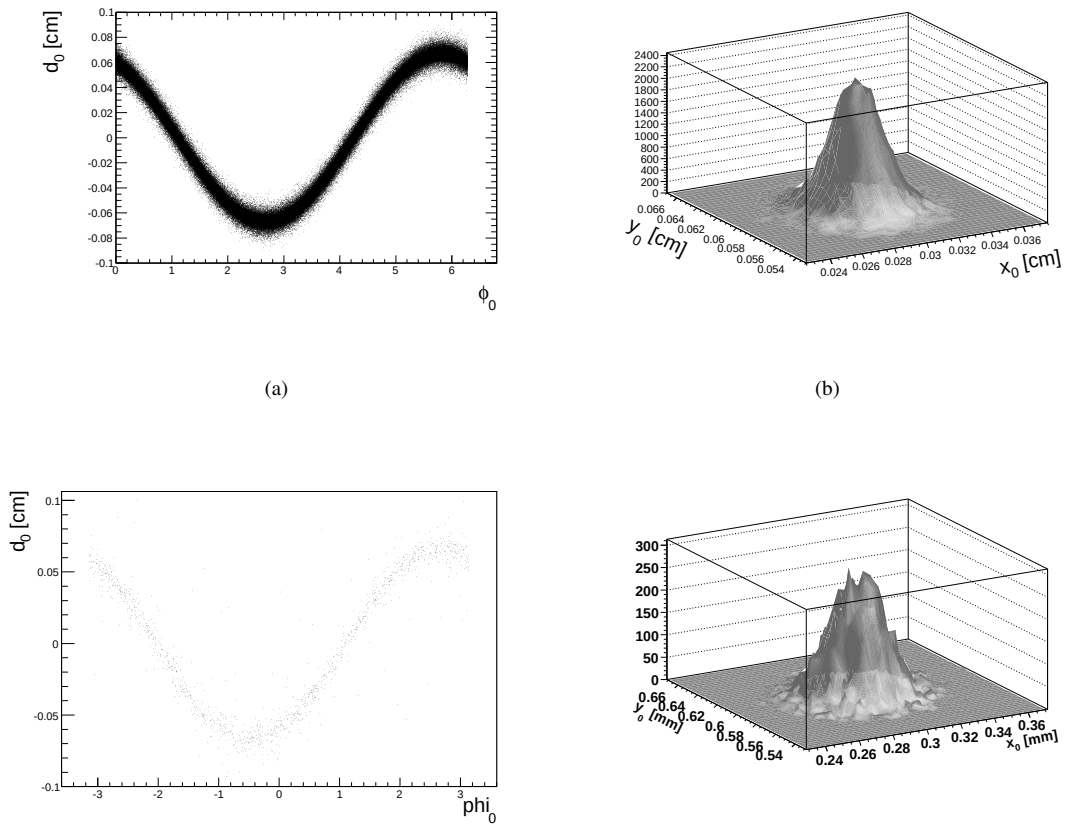

(a) (b)

(c) (d)

Figure 3: *(a) Correlation between d_0 and φ_0 for a displaced beam given by the stand alone generated sample. In this example the displacement of the beam with respect to the detector coordinate system is x_0 = 300 μm and y_0 = 600 μm (no slope in x and y). We observe a sine function where the amplitude is given by $\sqrt{x_0^2 + y_0^2} = 734$ μm and the phase is shifted by $\varphi_0 = tan\left(\frac{y_0}{x_0}\right) = 1.1$ radians. (b) Shows the transverse beam profile for the stand alone generated sample. (c) Correlation between d_0 and φ_0 for selected tracks from full simulation and reconstruction. (d) Transverse beam profile from the full simulation.*

and the vector $\vec{sg}$

$$sg_l = \sum_{i=1}^{N_{Tracks}} \frac{g_{li} \cdot d_{0i}}{\sigma_i^2}, \quad (l = 1, 2, 3, 4). \tag{8}$$

Tracks must initially pass a set of basic quality requirements. From this set, tracks that have a large contribution to the total χ^2 ($\Delta\chi^2 > \Delta\chi^2_{cut}$) or tracks which have a large impact parameter with respect to the fitted beam line ($|d_0'| > D_{cut}$) are removed until a given fraction of the tracks remain. All initially selected tracks are evaluated at each iteration. A track that was rejected in a previous iteration can enter the next iteration as the estimate of the beam position improves. In this way, no bias is introduced stemming from a bad initial fit. In this note an initial value D_{cut} = 4.0 cm was used, and this selection was tightened at each iteration, $D^{n+1}_{cut} = D^n_{cut}/1.5$, until about 50% of the initially selected tracks survive. The choice of this parameters is not optimized but also not very critical.

As more tracks are included in the fit, the convergence to the generated values is observed in Figure 4. A statistical precision of about 2 μm for x_0 and y_0 and ≈ 0.2 μm/cm for the slopes is achieved with 1000 tracks. This study was done using the fast parametrized Monte Carlo simulation with pixels described in Section 3.1.

The results of the $d_0 - \varphi_0$ fitter for different fully simulated and reconstructed samples consisting of 500 events each are shown in Table 4. In each case, the fit converges to a value within 2-3 μm of the value used to generate the sample.

Table 4: *Results of the $d_0 - \varphi_0$ fit for several fully simulated and reconstructed samples with 500 events, uncertainties are statistical only.*

Sample	Iteration	selected Tracks	x_0 [μm]	y_0 [μm]	dx/dz [$\times 10^{-6}$]	dy/dz [$\times 10^{-6}$]
generated values			0.0	0.0	0.0	0.0
QCD	1	6892	2.30 ± 0.67	2.17 ± 0.66	96.05 ± 12.87	61.92 ± 12.82
$(80 < \hat{p}_T < 120)$	19	4086	2.41 ± 0.94	-0.60 ± 0.92	44.22 ± 17.91	-19.98 ± 17.87
QCD	1	8824	2.06 ± 0.57	-0.11 ± 0.56	-10.44 ± 10.96	-38.23 ± 10.70
$(120 < \hat{p}_T < 170)$	19	5405	1.23 ± 0.77	-0.88 ± 0.76	-18.09 ± 15.11	-33.02 ± 14.54
b-jet	1	6392	0.56 ± 0.69	0.15 ± 0.68	233.78 ± 13.70	29.70 ± 13.26
$(50 < \hat{p}_T < 120)$	18	3431	-2.78 ± 1.06	2.38 ± 1.07	76.39 ± 21.34	-46.86 ± 20.64
QCD with PU	1	6933	-1.16 ± 0.74	-3.58 ± 0.74	95.05 ± 14.35	-35.69 ± 14.06
$(2 \times 10^{33} cm^{-2} s^{-1})$	19	3845	-0.57 ± 1.06	-1.02 ± 1.05	-35.08 ± 20.33	-20.41 ± 19.83
$(50 < \hat{p}_T < 80)$						
inclusive $t\bar{t}$	1	10802	7.45 ± 0.50	3.91 ± 0.49	27.78 ± 9.30	44.87 ± 9.21
	19	5680	-0.33 ± 0.75	0.43 ± 0.75	-12.94 ± 13.89	36.57 ± 14.09
generated values			300.0	600.0	2000.0	1000.0
QCD	1	2773	299.23 ± 1.01	592.55 ± 1.10	2004.07 ± 15.38	986.52 ± 16.42
$40 < \hat{p}_T$	19	1613	300.91 ± 1.39	601.41 ± 1.53	2023.38 ± 21.12	993.70 ± 23.01
generated values			300.0	600.0	150.0	0.0
QCD	1	2886	299.40 ± 1.05	600.48 ± 1.03	261.98 ± 15.83	-11.48 ± 15.72
$40 < \hat{p}_T$	19	1666	295.09 ± 1.51	599.13 ± 1.44	167.98 ± 22.35	-5.87 ± 21.86

Table 5: *Results of the $d_0 - \varphi_0$ fit for the fast simulation with and without pixel detector, uncertainties are statistical only. In the non pixel case, the p_t cut was raised to $p_t > 5$ GeV/c.*

Sample	Generated Tracks	x_0 [μm]	y_0 [μm]	dx/dz [$\times 10^{-6}$]	dy/dz [$\times 10^{-6}$]
generated values		300.0	600.0	0.0	0.0
with pixels	1000	299.59 ± 1.64	601.83 ± 1.74	-3.93 ± 22.32	-2.85 ± 25.76
with pixels	10000	299.98 ± 0.54	601.35 ± 0.54	-16.57 ± 7.08	3.36 ± 7.25
with pixels	20000	300.35 ± 0.38	600.57 ± 0.38	-2.00 ± 4.98	-5.39 ± 5.09
non pixels	1000	296.89 ± 7.50	605.53 ± 7.70	-77.29 ± 98.57	-132.54 ± 104.35
non pixels	10000	299.43 ± 2.38	597.03 ± 2.40	-34.80 ± 31.47	69.42 ± 32.03
non pixels	20000	299.42 ± 1.89	597.02 ± 1.90	12.83 ± 24.88	44.83 ± 25.36

The 90% confidence limits for the transverse position of the beam are shown in Figure 5 for the case with pixel

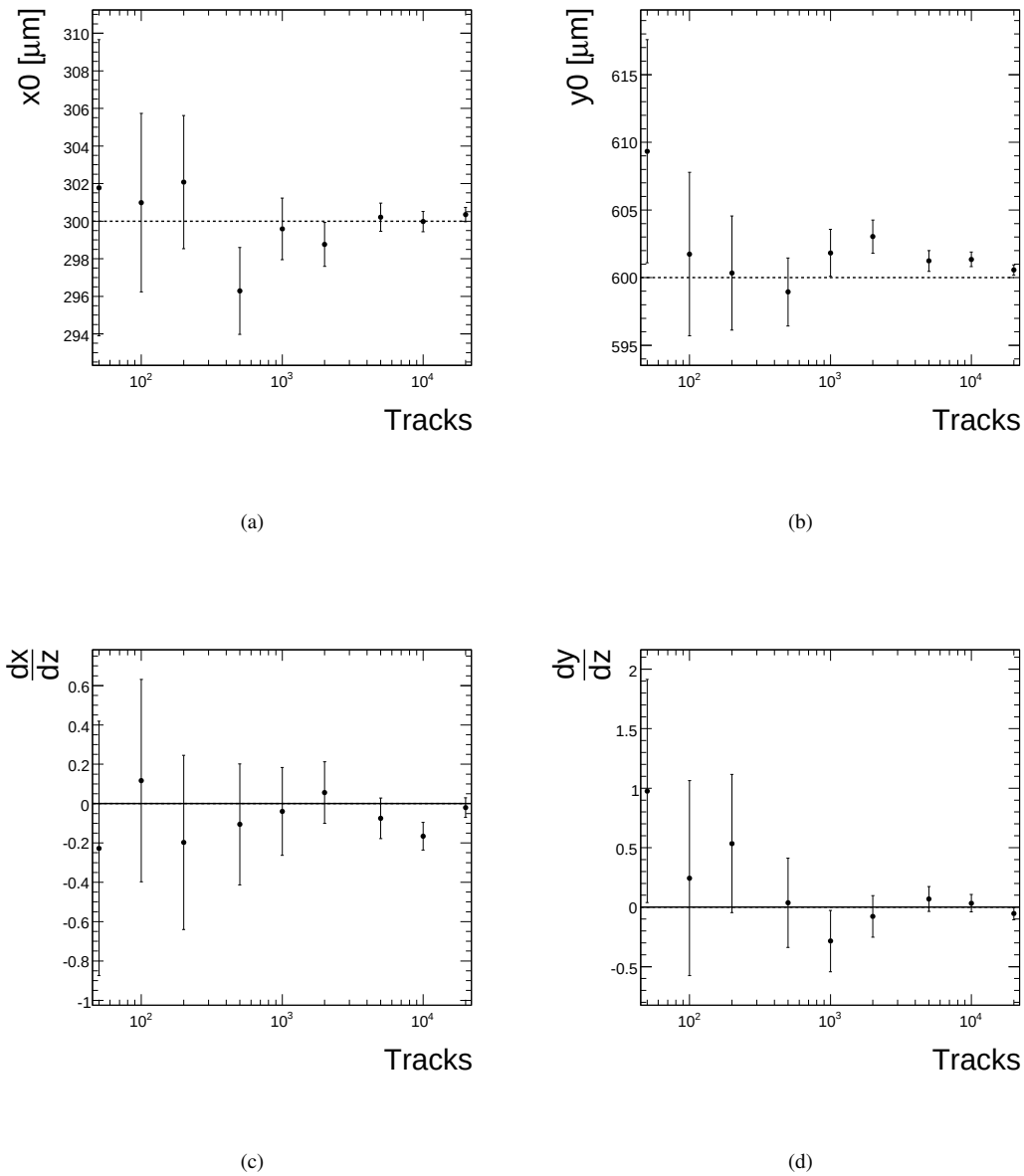

Figure 4: $d_0 - \varphi_0$ *fit results for (a)* x_0*, (b)* y_0*, (c)* $\frac{dx}{dz}$ *and (d)* $\frac{dy}{dz}$ *as a function of the number of tracks. Only 1000 tracks are needed to achieve a 2* μ*m statistical precision for the beam position. This study was done using the fast parametrized Monte Carlo simulation with pixels described in Section 3.1.*

(scenario 1) and for the case with no-pixel (scenario 2). The marker shows the input value used to generate the samples at (300,600,0) μm. For scenario (1), 20k tracks are used in the fit while 50k tracks and tightened p_T selection are required in scenario (2). In the non pixel case, the p_T cut was raised to $p_T > 5$ GeV/c. The average beam position can still be measured with worse resolution but the beam width cannot be resolved in this case. The results of the fit for both scenarios running only with the fast simulation is presented in Table 5.

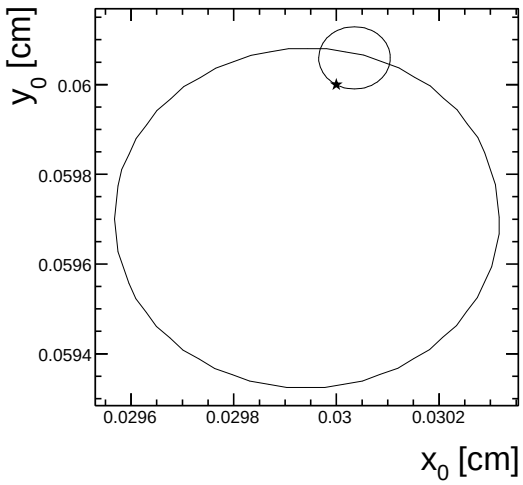

Figure 5: *90% CL contours for the transverse beam position with different IP resolutions. The marker shows the input value for the generation (300,600,0) μm. This study was done using the fast parametrized Monte Carlo simulation described in Section 3.1. The big ellipse with a radius of approximately 3 μm corresponds to the no-pixel case while the small ellipse with a radius of less than 1 μm corresponds to the case with pixel detector.*

5 Additional Beam Fitters

In the previous section, the $d_0 - \varphi_0$ fitter was shown to be robust, stable, and to yield good results. In this section, additional fitters are described. These fitters are extensions of the $d_0 - \varphi_0$ fitter providing additional information like the transverse beam width or the parameters of the β-function. These fitters are sensitive to several effects like the detector acceptance and require excellent understanding of the track parameter uncertainties, therefore only a proof-of-concept is given using the fast simulation. We only considered the detector configuration with pixels. Without pixels the resolution is not sufficient to extract the beam width and β function.

5.1 The Log-likelihood fitter to extract the beam parameters

To extract the beam parameters an unbinned log-likelihood fit can be used which treats the contribution of the track parameter errors to the probability function event by event. The probability function is the product of a longitudinal and a transverse component:

$$P(d_0', z_p, \sigma_{d0}^{tr}, \sigma_z^{tr}) = \frac{1}{\sqrt{2\pi}\sigma_{d'0}(z_p)} e^{-\frac{d_0'^2}{2\sigma_{d'0}(z)^2}} \cdot \frac{1}{\sqrt{2\pi}\sigma_z} e^{-\frac{(z_p - z_0)^2}{2\sigma_z^2}} \tag{9}$$

where d_0' is the impact parameter with respect to the beam given by

$$d_0' = d_0 - (x_0 + \frac{dx}{dz} z_p) \sin\varphi_0 + (y_0 - \frac{dy}{dz} z_p) \cos\varphi_0. \tag{10}$$

The error on d_0' is

$$\sigma_{d'0}(z_p) = \sqrt{(\sigma_{Beam})^2 + (\sigma_{d0}^{tr})^2}, \tag{11}$$

where σ_{d0}^{tr} is the impact parameter resolution of tracks as provided by the track fit. Assuming the transverse width of the beam does not vary much in z_p, as will be the case for the LHC nominal scenario, an average σ_{Beam} can be used. The error on z_p is

$$\sigma_z = \sqrt{(\sigma_z^b)^2 + (\sigma_z^{tr})^2}, \tag{12}$$

where σ_z^{tr} is the z resolution of tracks as returned by the track fit. This is small compared to the longitudinal width of the beam σ_z^b.

The likelihood function to be minimized is:

$$L = -2 \cdot \sum_i^{Tracks} \ln\left(P_i(d_0', z_p, \sigma_{d0}^{tr}, \sigma_z^{tr})\right), \tag{13}$$

where the measurements used in the fit are:

d_0', σ_{d0}^{tr}	:	impact parameter with respect to the beam and the error.
z_p, σ_z^{tr}	:	measured z of the track and error.
φ_0	:	direction of the track at the point of minimum approach.

The results of the fit (fit parameters) are:

x_0	:	center of the beam profile in the x axis.
y_0	:	center of the beam profile in the y axis.
$\frac{dx}{dz}$	:	x component of the beam slope.
$\frac{dy}{dz}$	:	y component of the beam slope.
z_0	:	center of the longitudinal Gaussian beam profile.
σ_{z_0}	:	longitudinal width of the beam.
σ_{Beam}	:	average beam width.

The minimization is done with `MINUIT` within the `ROOT` framework. Figure 6 shows how the fitted parameters converge to the correct input value. The results for the transverse position and slopes are, within errors, identical

to the $d_0 - \varphi_0$ fitter. A relative statistical precision of 20% for the beam width is achieved by using 1000 tracks. The results were obtained using the CMS tracking system with pixels and with beam parameters similar to those expected in the nominal LHC running conditions.

5.2 Fitting the β-function

This fit is the same as the one described in the previous Section 5.1, but instead of assuming a constant beam width, the width is allowed to vary with z according to Equation 1. Instead of one fit parameter σ_{Beam}, both the emittance ϵ and β^* are now fit. With beam conditions similar to the Tevatron, the CMS tracker with pixel detector would be able to provide a precise measurement of the beam profile in both longitudinal and transverse directions. Results for various beam scenarios, each based on approximately one million events, are given in Table 6. There are two problems with this fit:

- the parameters ϵ and β^* are highly correlated and there is a systematic tendency for the fitted β^* to be higher than the input value and the fitted ϵ to be lower. This requires a different parameterization of the beam profile, which does not have that problem.
- currently no detector acceptance effects are included. These could skew the probability function and would need to be corrected for.

In the nominal LHC scenario the transverse beam width is expected to vary very little over the interaction region justifying the use of a constant average transverse beam width as described in the previous subsection.

Table 6: *Beam Profile fitting results for CMS tracker with pixels. All samples consist of 950000 events and were generated with nominal z_0 at 0.0 cm.*

Input values			Fitted values			
σ_z $[cm]$	ϵ $[10^{-8}cm]$	β^* $[cm]$	z_0 $[cm]$	σ_z $[cm]$	ϵ $[10^{-8}cm]$	β^* $[cm]$
25	14	35	0.006 ± 0.026	24.70 ± 0.018	9.96 ± 0.06	44.37 ± 0.40
11.24	3.75	200	0.072 ± 0.012	11.232 ± 0.0083	2.67 ± 0.12	227.0 ± 10.3
7.55	3.75	55	0.0106 ± 0.0078	7.55541 ± 0.0055	3.38 ± 0.21	68.7 ± 4.5
7.55	1.0	55	0.0048 ± 0.0078	7.5443 ± 0.0055	0.97 ± 0.25	63.8 ± 16.5
7.55	6.0	55	0.048 ± 0.0078	7.543 ± 0.0055	4.69 ± 0.37	63.4 ± 5.2
7.55	3.75	25	0.0048 ± 0.0078	7.5437 ± 0.0055	3.49 ± 0.58	27.57 ± 5.28
7.55	3.75	75	0.0048 ± 0.0078	7.5443 ± 0.0055	2.83 ± 0.25	90.86 ± 8.02

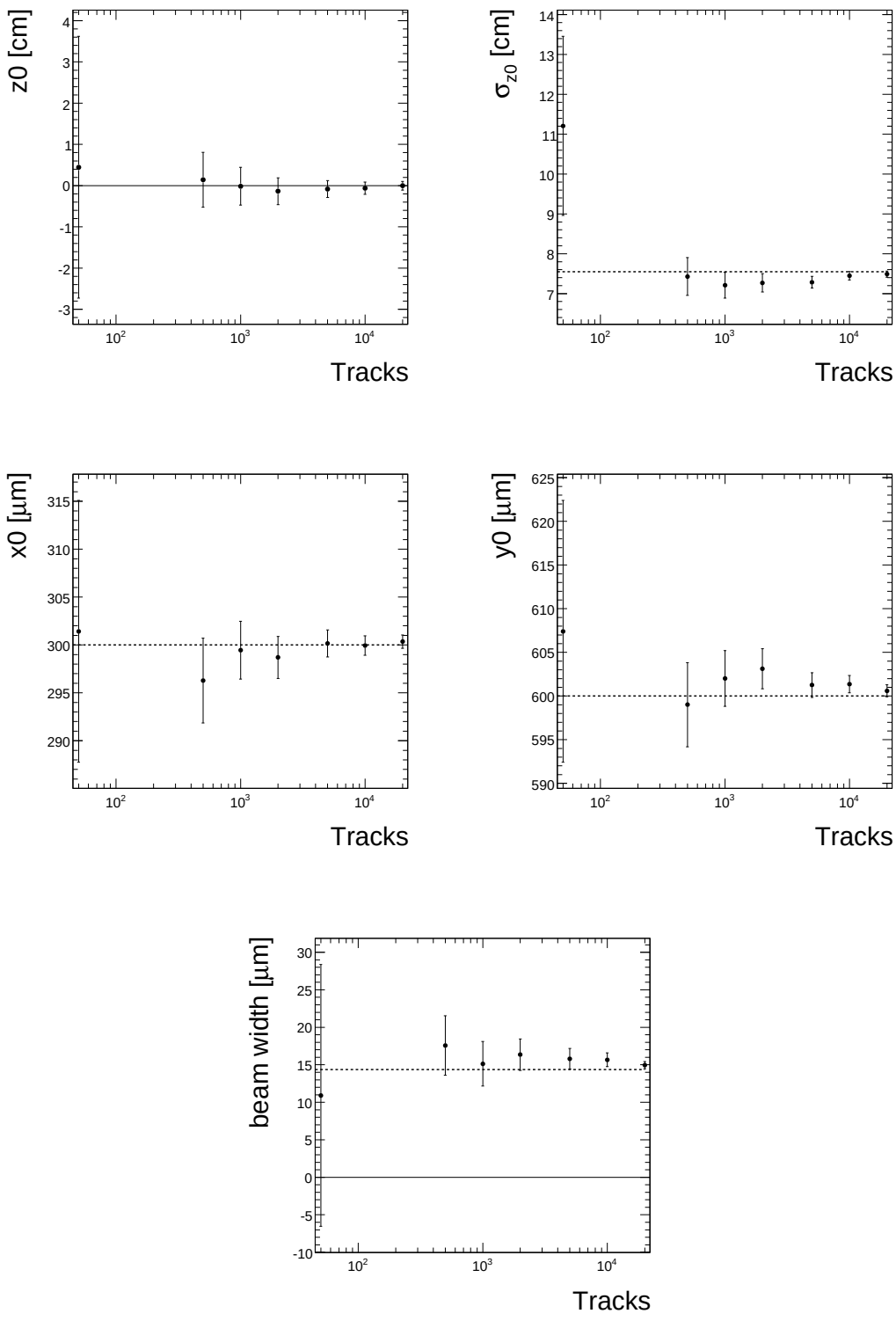

Figure 6: *Convergence of the likelihood fit for: the z_0 position and longitudinal width σ_{z_0} of the beam, the transverse x_0 and y_0 beam position, and the transverse beam width (σ_{Beam}). This study was done using the fast parametrized Monte Carlo simulation with pixels described in Section 3.1.*

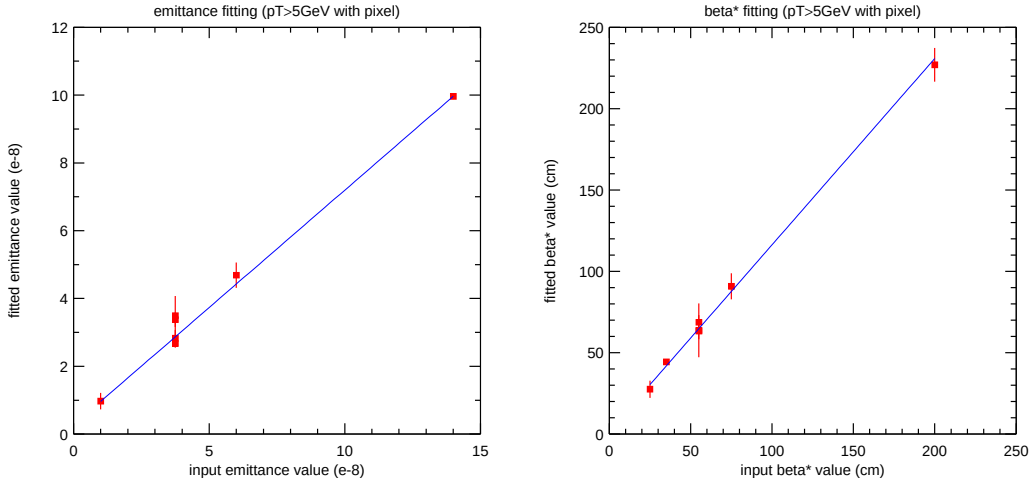

Figure 7: *Beam profile fit result with pixel in CMS. This study was done using the fast parametrized Monte Carlo simulation described in Section 3.1.*

6 Extracting the average Impact Parameter resolution function

The expected width of the LHC beam in the CMS interaction region is 16 μm and can be considered constant in z. This is smaller than the expected single track resolution even with the pixel system. This fact can be used to directly measure and monitor the average single track impact parameter resolution of the Tracker. The width of the impact parameter distribution with respect to the beam has two contributions: the width of the beam and the impact parameter resolution of the tracking detector. These two contributions behave very differently. While the beam width is constant, the impact parameter resolution is a function of the transverse momentum of the track. This fact helps to disentangle the two. In this Section, two studies are presented. The first study, based on the fast Monte Carlo simulation, uses the Log-likelihood fitter to extract the parameters of the impact parameter resolution function. The second study is based on the full simulation and reconstruction. In this study, the impact parameter and pull distributions for different bins in p_T are fitted to extract the impact parameter resolution function and to check the impact parameter uncertainty returned by the track fit. For both studies, the position and slope of the beam are first determined with high precision using the $d_0 - \varphi_0$ fitter. Then the track parameters are recalculated with the fitted beam as a new reference point. The uncertainty of beam position and slope given by the $d_0 - \varphi_0$ fit is small and can be neglected.

6.1 The Log-likelihood fitter to extract the Impact Parameter Resolution

Once all the beam parameters (position, slope and width) are well known they can be fixed, in the likelihood function described by Eq. (13), while the parameters c_0 and c_1 of the impact parameter resolution function Eq. (2) are allowed to vary. The values of c_0 and c_1 can then be extracted minimizing the likelihood function Eq. (13).

Using the fast parametrized Monte Carlo simulation, samples with different impact parameter resolutions were produced. The two impact Parameter resolution scenarios used to smear the generated tracks are:

1. $\sigma_{d0}^{tr}(p_T) = 10 + 90/p_T$ [μm] (as expected with pixels from full GEANT 4 simulation).
2. $\sigma_{d0}^{tr}(p_T) = 100 + 900/p_T$ [μm] (as expected without pixels from full GEANT 4 simulation).

The convergence of the likelihood fit for the c_0 and c_1 impact parameter resolution parameters are shown in Figure 8 for the scenario with pixels. The dotted lines represent the input value used to generate the sample. The case for a detector without pixels is shown in Figure 9.

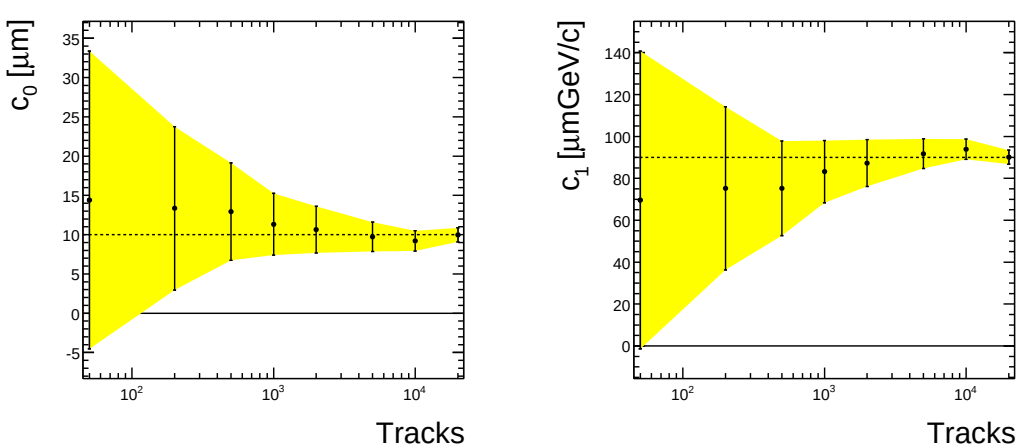

Figure 8: *Convergence of the likelihood fit for the c_0 and c_1 impact parameter resolution parameters, for impact parameter resolution scenario (1). This study was done using the fast parametrized Monte Carlo simulation with pixels described in Section 3.1.*

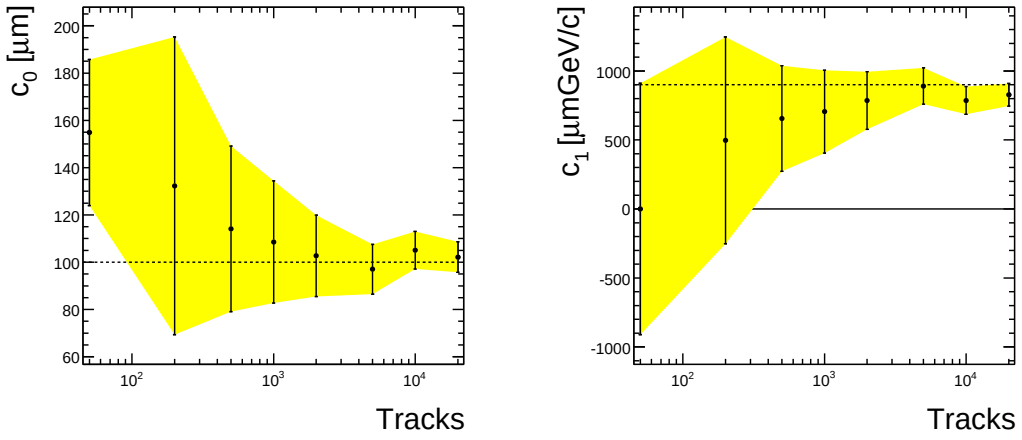

Figure 9: *Convergence of the likelihood fit for the c_0 and c_1 impact parameter resolution parameters, for impact parameter resolution scenario (2). This study was done using the fast parametrized Monte Carlo simulation with pixels described in Section 3.1.*

6.2 Measurement of the average Impact Parameter resolution from the full Monte Carlo simulation

All the results in this subsection are obtained using the full Monte Carlo simulation with pixels described in Section 3.2. First, the impact parameter d_0' (Eq. 10) is calculated in the beam reference frame and plotted for different p_T bins as shown in Figure 10. The distributions get narrower for higher p_T values as the contribution from multiple scattering decreases with p_T. These distributions are fitted to a Gaussian distribution function. The fact that the impact parameter resolution varies with the polar angle, as the track traverses more material, is not taken into account and the distributions are only approximately described by a Gaussian function. We use the σ of the Gaussian as an approximation of the impact parameter resolution averaged over all polar angles. As described in Equation 11, two components contribute to the width of this distribution, the transverse width of the beam, $\sigma_{Beam} = 16$ μm, and the impact parameter resolution of the tracker. So once the width of the beam is known one can extract the impact parameter resolution of the tracker: $\sigma_{d0}^{tr}(p_T) = \sqrt{(\sigma_{Distribution}(p_T))^2 - \sigma_{Beam}^2}$. This is plotted in Figure 11. The parameters of the resolution function are obtained by fitting this distribution with a linear function. The result of the fit is given on the same plot.

The normalized pull distributions $\frac{d_0'}{\sqrt{(\sigma_{d0}^{tr}(p_T))^2+\sigma_{Beam}^2}}$ are shown in Figure 12. These distributions are expected to be well described by a Gaussian distribution with a mean of 0 and a standard deviation σ of 1 and serve as a test that the impact parameter resolution as determined by the track fit is correct. Compared to the distributions in Figure 10 the normalized distributions should really be Gaussian since the impact parameter uncertainty returned by the track fit should include all effect like the polar angle dependence. In this case, the errors returned by the fit seem to be underestimated by 10 to 20% depending on track p_T (see Figure 13).

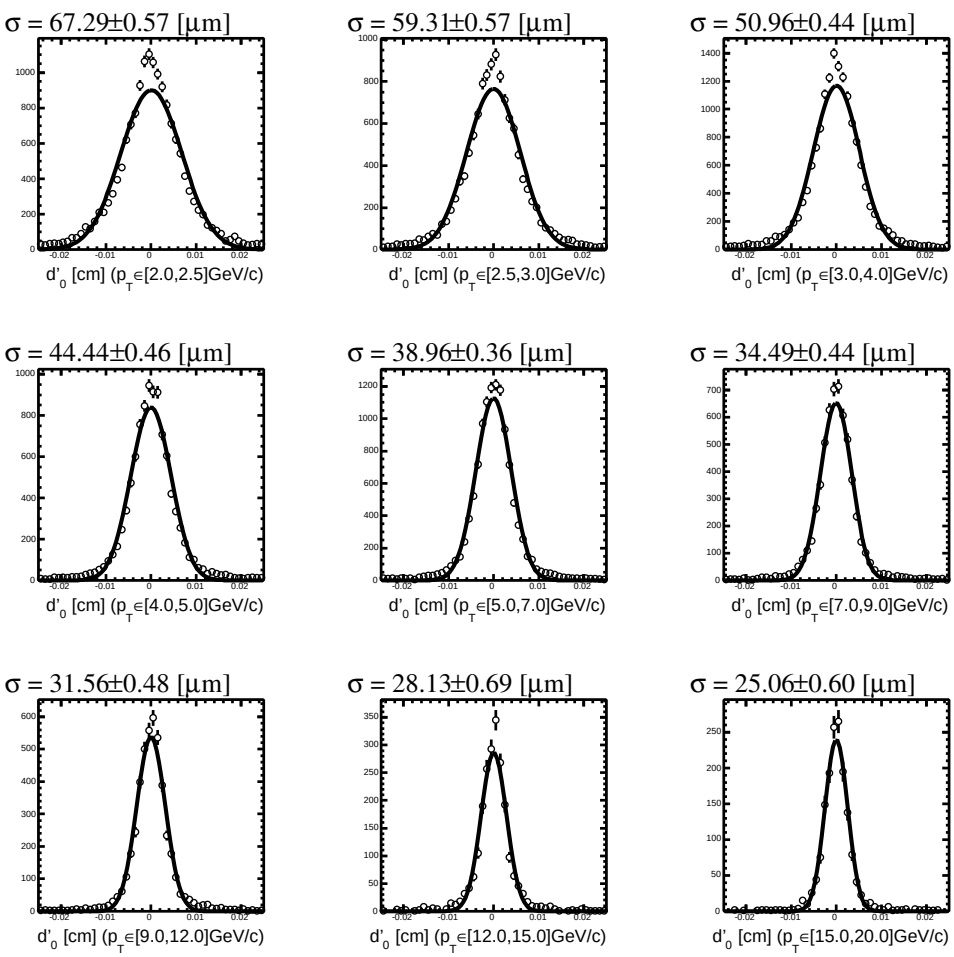

Figure 10: *Distribution of reconstructed d_0' (impact parameter in the beam reference frame, see 5.1) in bins of p_T obtained by the full MC simulation as described in 3.2. The track selection requirements are listed in Table 3.*

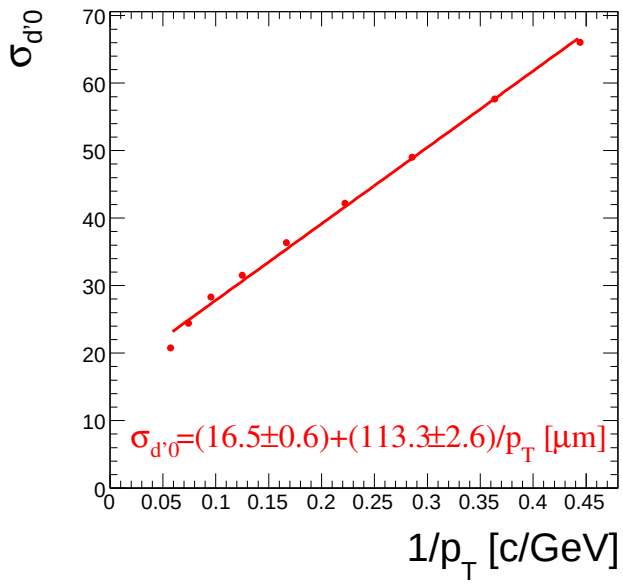

Figure 11: *Impact parameter resolution averaged over all polar angles as function of* $1/p_T$*. The solid line is the result of a linear fit. This result is obtained using the full MC simulation as described in Section 3.2.*

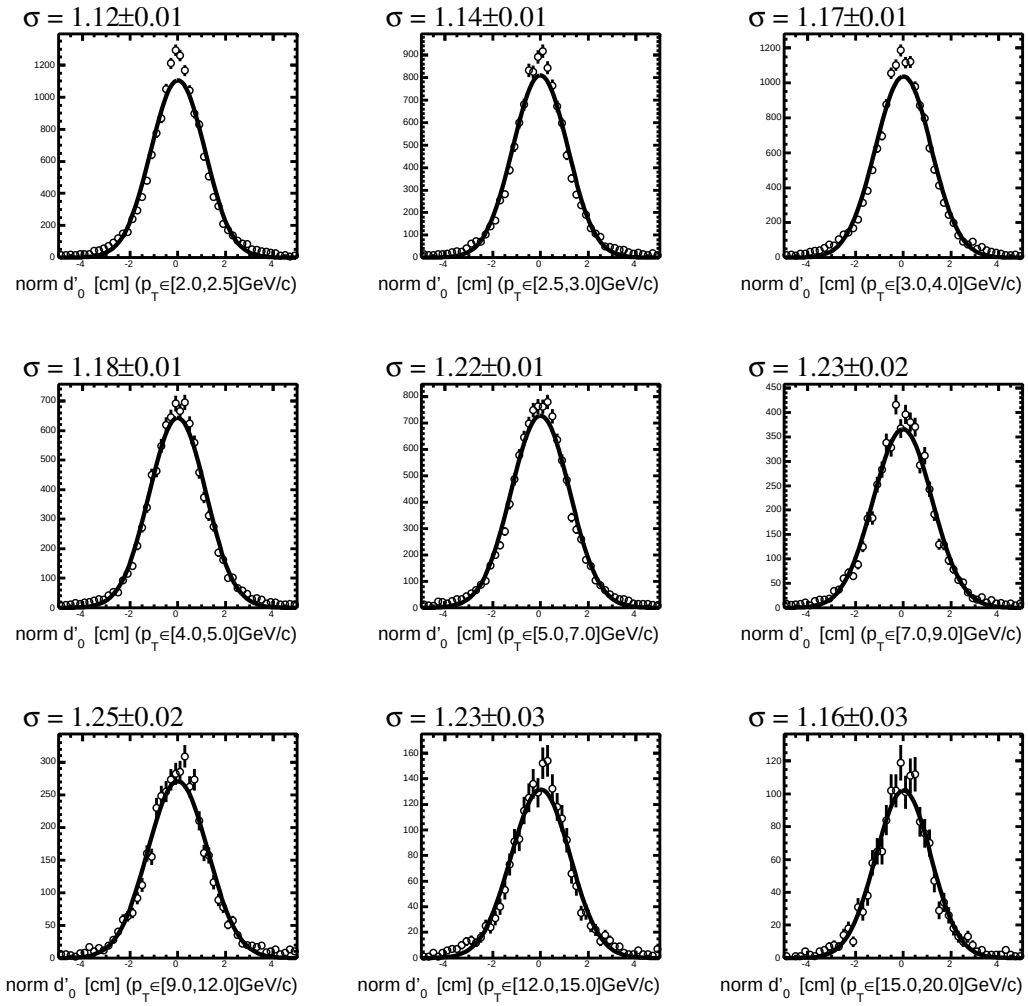

Figure 12: *Distribution of reconstructed* $\frac{d'_0}{\sqrt{\sigma^2_{d_0}+\sigma^2_{Beam}}}$ *(normalized impact parameter in the beam reference frame, see 5.1) in bins of* p_T *obtained by the full MC simulation as described in 3.2. The track selection requirements are listed in Table 3.*

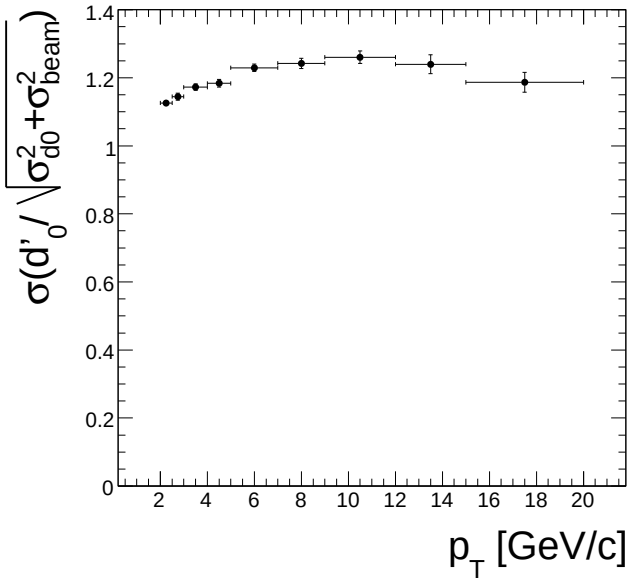

Figure 13: *Gaussian width for the impact parameter pull distributions as function of p_T. This result is obtained using the full MC simulation as described in Section 3.2.*

7 Conclusions

The work presented in this note shows that the beam position and width can be determined with algorithms based solely on track information. A statistical precision of 2 μm can be achieved for the average transverse beam position with only one thousand tracks that pass the selection criteria. Assuming that the beam width does not vary with z throughout the interaction region, it can also be measured with 20 % precision with the same track sample. The determination of the beam width requires good understanding of the impact parameter uncertainties as returned by the track fit.

The $d_0 - \varphi_0$ algorithm is fast and robust against large beam displacements. It allows the determination of the beam offsets and angles reasonably well without the pixel system, while the beam width, β^* and emittance require the tracking precision provided by the pixel detector. The $d_0 - \varphi_0$ fitter is ideally suited to monitor the beam during data taking as has been done by CDF for many years.

Once the beam parameters are determined with high precision this information can be used to study the track impact parameter resolution.

For the purpose of these studies the CMS detector simulation was expanded to include a more realistic simulation of the event vertex distribution. This included beam offsets in x, y and z from the nominal center of the detector; angles with respect to the detector z-axis and the interaction vertex to be distributed according to the β-function. The fit algorithms have been implemented in the CMS reconstruction software and an interface to write and read the beam spot data to and from the database has been developed.

8 Acknowledgments

We would like to thank Kevin Burkett, Hans Jensen and Lenny Spiegel (FNAL) for proof-reading this note. Thomas Speer, Jeff Spalding and Fabrizio served as referees and editor of this note. Hartmut Stadie (DESY) provided us with some of the C++ code. Francesco Ruggiero (CERN) provided us with references regarding the LHC beam parameters, we were saddened to hear the news that he passed away on the 17th of January.

Appendix 1

An additional check has been done varying the beam position over a wide range. This allows for displacement of several mm from the nominal detector coordinate system. Table 7 summarizes the results for a sample generated with the LHC nominal configuration. Table 8 shows the results for the case without pixel detector.

Table 7: *Beam Position fitting result with pixel in CMS tracker. Beam profile were generated using parameters* $\beta^* = 55\ cm$, $\epsilon = 3.75 \times 10^{-8}$ *and* $\sigma_z = 7.55\ cm$ *as expected for the nominal LHC stable runs. About 950K tracks with* $p_T > 2$ *GeV/c were used in each fit.*

Input values				Fitted values			
x_0 [μm]	y_0 [μm]	dx/dz [μm/cm]	dy/dz [μm/cm]	x_0(Fit) [μm]	y_0 (Fit) [μm]	dx/dz (Fit) [μm/cm]	dy/dz (Fit) [μm/cm]
0	0	0	0	0.110 ± 0.047	-0.004 ± 0.047	1.08 ± 0.63	1.15 ± 0.63
100	300	0	0	100.011 ± 0.047	300.006 ± 0.047	0.59 ± 0.63	-0.22 ± 0.63
300	600	0	0	299.982 ± 0.047	600.05 ± 0.047	0.02 ± 0.63	0.15 ± 0.63
600	900	0	0	600.064 ± 0.047	899.928 ± 0.047	0.43 ± 0.63	0.23 ± 0.63
900	1200	0	0	900.071 ± 0.047	1199.96 ± 0.047	-0.81 ± 0.63	-0.65 ± 0.63
1200	1500	0	0	1200.03 ± 0.047	1500.04 ± 0.047	0.15 ± 0.63	0.31 ± 0.63
1500	2000	0	0	1500.00 ± 0.047	1999.97 ± 0.047	-0.49 ± 0.63	-0.03 ± 0.63
2000	3000	0	0	1999.91 ± 0.047	3000.02 ± 0.047	0.13 ± 0.63	-0.35 ± 0.63
3000	4000	0	0	3000.03 ± 0.047	4000.04 ± 0.047	0.15 ± 0.62	-0.74 ± 0.63
4000	5000	0	0	3999.92 ± 0.047	4999.96 ± 0.047	0.08 ± 0.62	-0.40 ± 0.62
300	600	10	30	300.048 ± 0.047	599.938 ± 0.047	10.41 ± 0.63	30.14 ± 0.63
300	600	30	60	299.991 ± 0.047	599.907 ± 0.047	30.32 ± 0.63	60.13 ± 0.63
300	600	60	90	300.04 ± 0.047	600.012 ± 0.047	61.71 ± 0.63	91.65 ± 0.63
300	600	90	120	300.014 ± 0.047	599.949 ± 0.047	90.20 ± 0.63	120.25 ± 0.63
300	600	120	150	300.017 ± 0.047	599.975 ± 0.047	120.63 ± 0.63	150.78 ± 0.63
300	600	150	180	299.998 ± 0.048	599.983 ± 0.047	148.74 ± 0.63	179.35 ± 0.63
300	600	180	210	299.958 ± 0.048	599.985 ± 0.047	180.29 ± 0.63	209.73 ± 0.63

Table 8: *Beam Position fitting result using tracks from CMS detector configuration without pixel. Beam profile were generated using parameters* $\beta^* = 55\ cm$, $\epsilon = 3.75 \times 10^{-8}$ *and* $\sigma_z = 7.55\ cm$ *as expected for the nominal LHC stable runs. About 350K tracks with* $p_T > 5$ *GeV/c were used in each fit.*

Input values				Fitted values			
x_0 [μm]	y_0 [μm]	dx/dz [μm/cm]	dy/dz [μm/cm]	x_0(Fit) [μm]	y_0 (Fit) [μm]	dx/dz (Fit) [μm/cm]	dy/dz (Fit) [μm/cm]
0	0	0	0	0.03 ± 0.30	-0.63 ± 0.29	2.2 ± 3.9	2.9 ± 3.9
100	300	0	0	100.335 ± 0.30	300.05 ± 0.29	8.1 ± 3.9	-5.6 ± 3.9
300	600	0	0	300.33 ± 0.30	600.047 ± 0.29	3.1 ± 3.9	-3.4 ± 3.9
600	900	0	0	600.29 ± 0.30	899.969 ± 0.30	-1.7 ± 3.9	1.3 ± 3.9
900	1200	0	0	899.78 ± 0.30	1199.93 ± 0.29	-2.2 ± 3.9	1.9 ± 3.9
1200	1500	0	0	1200.04 ± 0.30	1499.89 ± 0.30	3.8 ± 3.9	1.3 ± 3.9
1500	2000	0	0	1500.31 ± 0.30	1999.65 ± 0.29	-3.0 ± 3.9	-4.0 ± 3.9
2000	3000	0	0	1999.93 ± 0.30	3000.4 ± 0.29	4.2 ± 3.9	-0.3 ± 3.9
3000	4000	0	0	3000.24 ± 0.30	3999.98 ± 0.29	-3.0 ± 3.9	6.2 ± 3.9
4000	5000	0	0	3999.76 ± 0.30	4999.94 ± 0.29	4.6 ± 3.9	-2.8 ± 3.9
300	600	10	30	300.60 ± 0.30	599.941 ± 0.29	17.2 ± 3.9	29.9 ± 3.9
300	600	30	60	300.04 ± 0.30	599.881 ± 0.29	33.0 ± 3.9	59.9 ± 3.9
300	600	60	90	300.03 ± 0.30	599.641 ± 0.29	65.9 ± 3.9	87.1 ± 3.9
300	600	90	120	299.97 ± 0.30	599.827 ± 0.29	89.9 ± 3.9	120.2 ± 3.9
300	600	120	150	300.44 ± 0.30	599.847 ± 0.29	127.4 ± 3.9	153.1 ± 3.9
300	600	150	180	299.83 ± 0.30	600.491 ± 0.29	146.2 ± 3.9	177.6 ± 3.9
300	600	180	210	299.97 ± 0.30	599.623 ± 0.29	179.1 ± 3.9	208.9 ± 3.9

Appendix 2

Below are the PYTHIA control cards for minimum bias events and for QCD events with minimal parton E_T of 50 GeV/c.:

pythia− >SetMSEL(1); // select all processes (aka Min Bias)
pythia− >SetMSTP(51,7); // select CTEQ 5L structure function
pythia− >SetMSTP(81,0); // switch off mutiple interactions
pythia− >SetMSTJ(22,2); // Decay those unstable particles
*pythia− >SetPARJ(71,10.); // for which c*tau < 10 mm;*
pythia− >SetMSTP(33,3); // include k-factor
pythia− >SetPARP(82,3.20); // cut-off pt for multiple interaction
pythia− >SetPARP(89,1960.);
pythia− >SetMSTJ(11,3); // select fragmentation function "Bowler"
pythia− >SetMSTP(61,1); // master switch for initial state QED and QCD ra diation
pythia− >SetMSTP(71,1); // master switch for fi nal state QED and QCD ra diation
// uncomment the next 2 line line to set kinematic cuts:
//pythia− >SetCKIN(3,50.);
//pythia− >SetKSEL(0);
pythia− >Initialize("cms", "p", "p", 14000);

References

[1] CERN/LHCC 2006-001, CMS Physics TDR Vol 1.

[2] There are many examples where the beam was used as an estimate for the primary interaction vertex. Two examples are:
"Measurement of the Average Lifetime of B hadrons produced in $\bar{p}p$ collisions at $\sqrt{s} = 1.8$ TeV", F. Abe *et al.*, The CDF Collaboration, Phys. Rev. Lett. **71**, 3421 (1993).

"Measurement of B Hadron Lifetimes Using J/ψ Final States at CDF", F. Abe *et al.*, The CDF Collaboration, Phys. Rev. **D57**, 5382 (1998).

[3] "The Silicon Detector of the Collider Detector at Fermilab." Nuclear Instruments and methods in Physics Research A 350 (1994) p 73-130.

[4] "CDF Run 2A Silicon Detector Damage. Assessment." G. Bolla et al.
"http://www-cdf.fnal.gov/upgrades/run2b/P5_Mar03/damage.ps"

[5] Beam Physics Note 63 25/04/02, B. Muratori, *"Luminosity Considerations for the LHC".*

[6] W. Herr, B. Muratori, *"Concept of Luminosity".* Prepared for CERN Accelerator School and DESY Zeuthen: Accelerator Physics, Zeuthen, Germany, 15-26 Sep 2003 "http://lhc-beam-beam.web.cern.ch/lhc-beam-beam/papers/lum.ps"
"http://cas.web.cern.ch/cas/Trieste-2005/Lectures-pdf/Herr-luminosity.pdf".

[7] "Tevatron Run II Luminosity, Emittance and Collision Point"
J. Slaughter, J. Estrada, K. Genser, A. Jansson, P. Lebrun, J. C. Yun, S. Lai
Particle Accelerator Conference, 2003. PAC 2003. Proceedings of the Volume 3, Issue , 12-16 May 2003 Page(s): 1763 - 1765 Vol. 3.

[8] B. Mangano, "The CMS Tracker: contributions to hardware integration, software development and first data taking", Ph.D. thesis in preparation.

[9] V. Shiltsev *et al.*, Phys. Rev. ST Accel. Beams 8, 101001 (2005).

[10] RUN II Handbook "http://www-bd.fnal.gov/runII/index.html".

[11] "http://lhc.web.cern.ch/lhc/" under "Beam Parameter".

[12] "http://root.cern.ch/root/html/TPythia6.html".

[13] T. Sjostrand, L. Lonnblad, and S. Mrenna, "PYTHIA 6.2: Physics and manual", arXiv:hep-ph/0108264. "http://www.thep.lu.se/ torbjorn/Pythia.html".

[14] W. Adam et al., "Track reconstruction in the CMS tracker", CMS Note 2006/041 (2006).

[15] IOMC/EventVertexGenerators package within the CMS software reconstruction,

"http://cmssw.cvs.cern.ch/cgi-bin/cmssw.cgi/CMSSW/IOMC/EventVertexGenerators/?cvsroot=CMSSW".

[16] The $d_0 - \varphi_0$ and log-likelihood fits have been implemented in a package within the CMS software reconstruction. This package also includes a class object (BeamSpot) that holds all the beam information: XYZ beam position, two slopes, RMS beam length, beam width, and a full covariance matrix. This object can be used to store the beam information in the database. The fits available are: χ^2 and log-likelihood fits for z-distribution, $d_0 - \varphi_0$ fitter, log-likelihood fit for beam position and log-likelihood fit for extraction of the beam width. The likelihood fitters have been implemented using MINUIT2.

[17] "http://cdcvs.fnal.gov/cgi-bin/public-cvs/cvsweb-public.cgi/beamfit/?cvsroot=lpc".

[18] M. Vos and F. Palla, "b-tagging in the High Level Trigger", CMS Note 2006/030 (2006).